The Use of RBF Neural Network to Predict Building's Corners Hygrothermal Behavior

Roberto Z. Freire[1,†,*]; Leandro dos S. Coelho[1,†]; Gerson H. dos Santos[3], Viviana C. Mariani[2,†]; Nathan Mendes[2,†]; and Divani da S. Carvalho[1,†]

†- Pontifical Catholic University of Parana (PUCPR) - Polytechnic School
Rua Imaculada Conceição, 1555. Postal Code: 80215-901, Curitiba, Brazil
1- Industrial and Systems Engineering Graduate Program (PPGEPS)
2- Mechanical Engineering Graduate Program (PPGEM)
3- Federal Technological University of Parana - Department of Mechanical Engineering
Av. Monteiro Lobato, Km 04, Postal Code: 84016-210, Ponta Grossa, Brazil

Abstract. In this paper, a radial basis function neural network (RBF-NN) was combined with two optimization techniques, the expectation-maximization clustering method was used to tune the Gaussian activation functions centers, and the differential evolution was adopted to optimize the spreads and to local search of the centers. The modified RBF-NN was employed to predict building corners hygrothermal behavior. These specific regions of buildings are still barely explored due to modelling complexity, high computer run time, numerical divergence and highly moisture-dependent properties. Moreover, these specific building areas are constantly affected by moisture accumulation and mould growth, conditions that favor structure damages.

1. Introduction

In Brazil, buildings from residential, commercial and public sectors are responsible for at least 45% of the total energy demand [1]. The amount of energy attributed to buildings motivated the Brazilian government to create a certification program to avoid energy waste. According to the Brazilian' laws, it is possible to estimate the energy demand of buildings by using a validated software based on a set of analytical and empirical models to describe the building energy and thermal behavior [2].

Most of building simulation software that are capable to perform this type of energy consumption evaluation do not take into account the moisture presence. The presence of moisture in building porous elements can imply an additional mechanism of transport absorbing or releasing latent heat of vaporization, causing mold growth and structural damage (Fig. 1 (a) and (b)) [3]. Associated to these problems, thermal comfort and energy consumption can be significantly affected by excessive moisture presence, by changing the heat insulation capacity of the building materials.

However, when both multidirectional and coupled heat and moisture transfer calculations are considered in building simulation, it becomes hardware- and time-consuming due to numerical divergence and highly moisture-dependent properties. In this way, the whole building simulation is always restricted to some regions that are not considered important in the moisture presence analysis. The important regions are the corners (or thermal bridges) of the building envelop.

In order to provide a faster and a more precise model capable to simulate thermal bridges coupled to the whole building simulation considering the moisture presence, this paper presents a modified Radial Basis Function Neural Network (RBF-NN) which uses two optimization techniques – Expectation Maximization clustering and Differential Evolution - to estimate the heat, moisture and vapor transfer in buildings' thermal bridges. The RBF-NN was trained, tested and validated by using data provided by a multidimensional model proposed in [3]. This analytical model was used to generate data that represents the hygrothermal behavior of the building corners (Fig. 01 (c)) that were adopted as inputs for the creation of six MISO models that could represent the hygrothermal behavior of the thermal bridges in a faster and easier way.
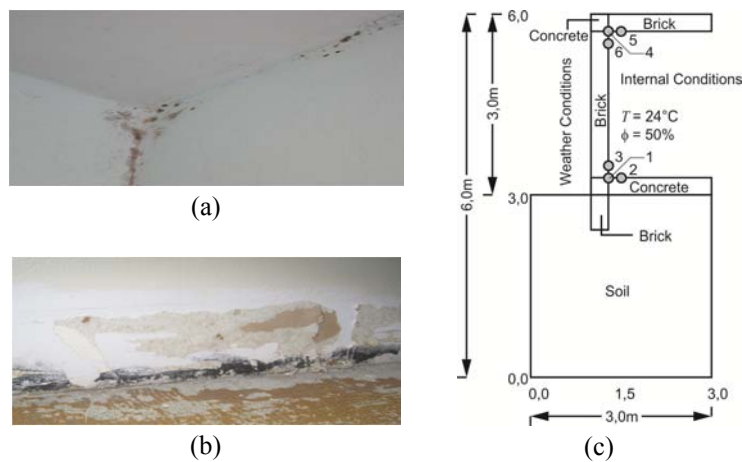

(a)

(b)

(c)

Fig. 1: (a) Mould growth at the upper corner; (b) Structural damage at the lower corner, different materials; (c) Physical domain of the lower and upper corners.

The next section of this work presents the analytical model used to generate data for both RBF-NN estimation and validation phases. In the sequence, section 3 addresses the system identification technique and shows the modifications on the RBF-NN parameters by using two optimization methods. Section 4 describes the identification procedures and results. Finally, the conclusions about this work and future research are presented in section 5.

2. Porous media analytical model: thermal bridges

The model capable to simulate the hygrothermal performance of building corners considers the differential governing equations for moisture, air and energy balances through the building surfaces [3,4].

The moisture transport can be divided into liquid and vapor flows, and the moisture content conservation equation can be expressed in terms of the three driving potentials. The dry air transport can be described as a function of the partial gas and vapor pressure driving potentials and the air balance. The heat transfer can be written in terms of both conductive and convective effects. According to [3,4], the moisture

transport can be divided into liquid and vapor flows, and the moisture content conservation equation can be written in terms of the three driving potentials as:

$$\frac{\partial w}{\partial \phi}\frac{\partial \phi}{\partial P_v}\frac{\partial P_v}{\partial t} + \frac{\partial w}{\partial \phi}\frac{\partial \phi}{\partial T}\frac{\partial T}{\partial t} = \nabla \begin{bmatrix} -K\frac{\partial P_{suc}}{\partial T}\nabla T - \left(K\frac{\partial P_{suc}}{\partial P_v} - \delta_v\right)\nabla P_v \\ \\ +\rho_v \frac{kk_{rg}}{\mu_g}\nabla P_g + K\rho_l g \end{bmatrix} \quad (1)$$

where w is the moisture content (kg/m³), ϕ, the relative humidity (-), P_v, the partial water vapor pressure (Pa), T, the temperature (K), t, is the time (s), K, the liquid water permeability (s), P_{suc} the suction pressure (Pa), ρ_l the liquid water density (kg/m³) , g, the gravity (m/s²), δ_v, the vapor diffusive permeability (s), ρ_v, the water vapor density (kg/m³), k, the absolute permeability (m^2), k_{rg}, the gas relative permeability, μ_g, the dynamic viscosity (Pa.s) and, P_g, the gas pressure - dry air pressure plus vapor pressure (Pa). The air transport is individually considered through the dry-air mass balance. In this way, the dry air transport can be described as a function of the partial gas and vapor pressure driving potentials and the air balance can be written as:

$$\frac{\partial \rho_a}{\partial P_g}\frac{\partial P_g}{\partial t} + \frac{\partial \rho_a}{\partial P_v}\frac{\partial P_v}{\partial t} + \frac{\partial \rho_a}{\partial T}\frac{\partial T}{\partial t} = \nabla\left(-\delta_v \nabla P_v + \rho_a \frac{kk_{rg}}{\mu_g}\nabla P_g\right) \quad (2)$$

where ρ_a is the density of dry air (kg/m^3).

The heat transfer can be written in terms of both conductive and convective effects. Assuming 0°C as the reference temperature, the energy conservation equation can also be described in terms of the three driving potentials as:

$$c_m \rho_0 \frac{\partial T}{\partial t} = \nabla \begin{bmatrix} \left(\lambda - K\frac{\partial P_{suc}}{\partial T}c_{pl}T\right)\nabla T - \begin{pmatrix} K\frac{\partial P_{suc}}{\partial P_v}c_{pl}T - \delta_v c_{pa}T \\ -\delta_v(L + c_{pv}T) \end{pmatrix}\nabla P_v \\ \\ +\left(\rho_a \frac{kk_{rg}}{\mu_g}c_{pa}T + \rho_v \frac{kk_{rg}}{\mu_g}(L + c_{pv}T)\right)\nabla P_g + K\rho_l c_{pl}Tg \end{bmatrix} \quad (3)$$

where c_m is the specific heat capacity of the structure (J/kgK), ρ_0, the density of the dry material (kg/m³), λ, the thermal conductivity (W/mK), c_{pl}, the specific heat capacity of the water liquid (J/kgK), c_{pa}, the specific heat capacity at constant pressure of the dry air (J/kgK), c_{pv}, the specific heat capacity at constant pressure of the vapor (J/kgK) and, L, the vaporization latent heat (J/kg). As boundary conditions, the gas pressure was considered as a prescribed value at the envelope surface according to Dirichlet condition. The vapor transport was defined due to the difference between the partial vapor pressure in the air and at the external and internal surfaces. For the heat transport, convection heat transfer and phase change were also considered. To solve these highly coupled equations, the MTDMA [5] algorithm was adopted to calculate the solution at each time step (600s in this work). Data were collected for a whole year simulation period that has taken 14 days to be concluded.

3. Modifications on the Radial-Basis Function Neural Network

RBF-NN is a special three-layered ANN (Artificial Neural Networks), which has widely been applied to thermal process [6-8]. According to [9], the mapping process from input to output can be viewed as a function in the input space. In these case, learning may be described as a function approximation problem, where providing the best fit to training data means finding a surface in a multidimensional space. A symmetrical Gaussian function was used at the output of the hidden neurons [10,11].

The RBF-NN design was combined with Expectation-Maximization (EM) clustering to tune the Gaussian activation functions centers and Differential Evolution (DE) to optimize the spreads and to realize the local search of the centers provided by EM. The DE algorithm [12] uses mutation as a search mechanism and selection to direct the search toward the prospective regions in the search space. In DE, the difference vector, which is defined by each individual pair in a population, plays an important part in the generation of the mutant vector. Moreover, the crossover operation of the DE is used to strengthen the exploitation ability of the algorithm.

EM is an iterative algorithm for finding maximum likelihood or maximum values, it estimates the parameters in statistical models that are adopted in problems where data are incomplete or sometimes considered incomplete. The algorithm can be divided into two stages [13], namely the initialization stage and the iterative stage, where the last one consists of two steps: *i*) the expectation step (E-step) which creates a function for the expectation of the log-likelihood evaluated using the current estimation for the parameters; and *ii*) the maximization step (M-step), which computes parameters maximizing the expected log-likelihood found on the E-step.

4. Identification Procedures and Results

The simulation was performed by using the model presented in section 2 and the physical domain of Fig. 1 (c). The six nodes used on the identification procedures are indicated by grey circles (394,241 nodes were simulated in order to provide convergence for the analytical model. As initial conditions for the whole domain, temperature, relative humidity and gas pressure of 293 K, 60% (humid condition) and 100 kPa have been assumed. Internally, at the upper surface of the floor and right surface of the wall, constant uniform values of 3 W/m²K, 297 K and 50% have been considered for the convective heat transfer coefficient, temperature and relative humidity, respectively, for an air conditioned environment. The other surfaces have been considered adiabatic and impermeable. External weather conditions for Curitiba city (Brazil) were adopted in this work.

The mathematical model employed in this work is a Nonlinear AutoRegressive with eXogenous inputs (NARX) model with MISO structure. In this case, the NARX model with series-parallel conception is used for one-step ahead prediction using the RBF-NN. The inputs data adopted in the RBF-NN model are: the outdoor temperature $u_1(t)$, in K, and the outdoor relative humidity $u_2(t)$ (-). The notations for the estimated output of RBF-NN (see Table 1) are: k, the number of radial basis functions of RBF-NN's hidden nodes, "^", the estimated output provide by the RBF-NN, where the variable without "^" is the measured (real) output, $\hat{y}_1(t)$, the estimated node temperature in K, $\hat{y}_2(t)$, the estimated vapor pressure in the node in Pa, and $\hat{y}_3(t)$, the

164

estimated relative humidity of the node. The multiple correlation coefficient R^2 presented in equation 4 was used to quantify the goodness of the models, where Ns is the number of samples used for estimation and validation phases.

$$R^2 = 1 - \frac{\sum_{t=1}^{Ns}[y(t) - \hat{y}(t)]^2}{\sum_{t=1}^{Ns}[y(t) - \bar{y}(t)]^2} \qquad (4)$$

The setup used for DE was the following: crossover rate equal to 0.8, mutation factor of 0.8, population size of 15, and stopping criterion of 40 generations. Table 1 presents the RBF-NN results for the most critical nodes #1 and #4, by designing two Gaussian activation functions for each input. As it can be verified in Table 1, the modified RBF-NN provided MISO models that are capable to predict temperature, vapor pressure and relative humidity considering the values of R^2 obtained for the validation procedure. The best results for node #1 are presented in Fig. 2, where the error associated to both estimation and validation phases are reported. The errors provide by the model are quite small and considered acceptable in terms of slow thermal systems, providing mean differences smaller than 0.1K, 5Pa and 0.01% for temperature, vapor pressure and relative humidity respectively.
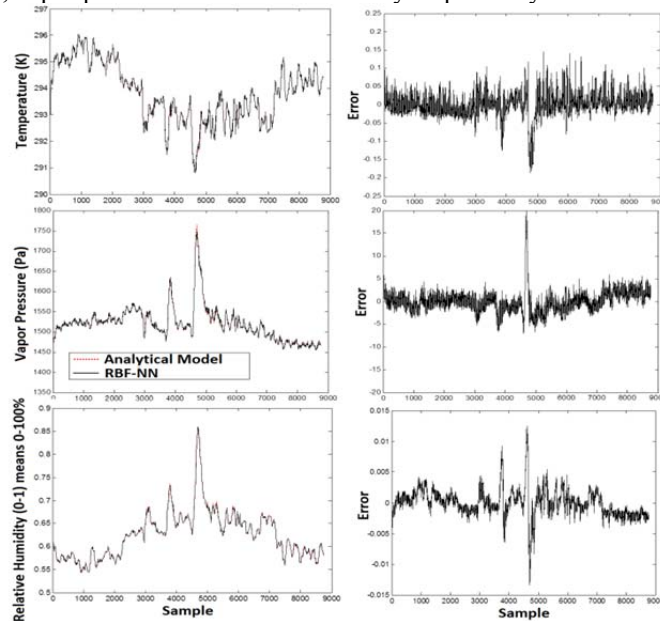

Fig. 2: Best results using RBF-NN with EM and DE for the node #1.

5. Conclusion

The performance of a modified RBF-NN design combining EM and DE has been evaluated by using the prediction of hygrothermal behavior of thermal bridges in buildings through a NARX model with MISO structure. The results reveal that RBF-NN offers a promising performance in terms of the solution quality and simulation time for hygrothermal systems. Future work is aimed at including the prediction of mould growth risk based on temperature, vapor pressure and relative humidity. The additional output will be added to the model and it will be integrated into a building

simulation tool due to its fast prediction when compared to the analytical model. Finally, the *n*-steps approach will also be discussed.

Node	Input vector	Predicted output	R^2_{est} maximum	R^2_{est} mean	R^2_{val} mean
1	$[u_1(t\text{-}1), u_2(t\text{-}1), y_2(t\text{-}1), y_3(t\text{-}1)]$	$\hat{y}_1(t)$	0.9994	0.9939	0.9652
1	$[u_1(t\text{-}1), u_2(t\text{-}1), y_1(t\text{-}1), y_3(t\text{-}1)]$	$\hat{y}_2(t)$	0.9913	0.8811	0.9477
1	$[u_1(t\text{-}1), u_2(t\text{-}1), y_1(t\text{-}1), y_2(t\text{-}1)]$	$\hat{y}_3(t)$	0.9982	0.9978	0.9969
4	$[u_1(t\text{-}1), u_2(t\text{-}1), y_2(t\text{-}1), y_3(t\text{-}1)]$	$\hat{y}_1(t)$	0.9995	0.9955	0.9875
4	$[u_1(t\text{-}1), u_2(t\text{-}1), y_1(t\text{-}1), y_3(t\text{-}1)]$	$\hat{y}_2(t)$	0.9804	0.9219	0.9279
4	$[u_1(t\text{-}1), u_2(t\text{-}1), y_1(t\text{-}1), y_2(t\text{-}1)]$	$\hat{y}_3(t)$	0.9970	0.9958	0.9901

Table 1. Prediction results of the RBF-NN with EM and DE (in 30 runs).

References

[1] Ministry of Mines and Energy – MME (Brazil). *National Energy Balance 2013* (i*n Portuguese*), 2014.

[2] National Institute of Metrology, Quality and Technology - INMETRO. T*echnical Requirements of Quality for Energy Efficiency of Public, Commercial and Service Buildings* – RTQ–C, Brazil (*in Portuguese*), 2010.

[3] G. H. Santos and N. Mendes, Corner effects on the hygrothermal performance of buildings, In *proceedings of the 13th Building Simulation Conference* (BS 2013), IBPSA, pages 3546-3553, Chambéry, France, 2013.

[4] G. H. Santos and N. Mendes. A building corner model for hygrothermal performance and mould growth risk analyses, *International Journal of Heat and Mass Transfer*, 52:4862-4872, Elsevier, 2009.

[5] N. Mendes, P. C. Philippi and R. A. Lamberts, New mathematical method to solve highly coupled equations of heat and mass transfer in porous media, *International Journal of Heat and Mass Transfer*, 45:509-518, Elsevier, 2002.

[6] A. Sridhar, A. Vincenzi, M. Ruggiero and D. Atienza. Neural network-based thermal simulation of integrated circuits on GPUs, *IEEE Transactions on Computer-Aided Design of Integrated Circuits and Systems*, 31:23-36, IEEE, 2012.

[7] S. Li, S. Ren, X. Wang. HVAC room temperature prediction control based on neural network model, In *proceedings of the 5th International Conference on Measuring Technology and Mechatronics Automation* (ICMTMA 2013), pages 606-609, Hong Kong, China, 2013.

[8] W. Dong, Z. Long and L. Xi. Research on neural network based real-time thermal load prediction, In *proceedings of the International Conference on Electrical and Control Engineering* (ICECE), pages 1718-1720, Dhaka, Bangladesh, 2010.

[9] N. B. Karayiannis and G. W. Mi, Growing radial basis neural networks: merging supervised and unsupervised learning with network growth techniques, *IEEE Transactions on Neural Networks*, 8:1492-1506, IEEE, 1997.

[10] L. S. Coelho, R. Z. Freire, G. H. dos Santos, and N. Mendes. Identification of temperature and moisture content fields using a combined neural network and clustering method approach, *International Communications in Heat and Mass Transfer*, 36:304-313, Elsevier, 2009.

[11] J. Yin, Z. Zou and F. Xu. Sequential learning radial basis function network for real-time tidal level predictions, *Ocean Engineering*, 57:49-55, Elsevier, 2013.

[12] R. Storn and K. Price, Differential evolution - A simple and efficient heuristic for global optimization over continuous spaces, *Journal of Global Optimization*, 11, (4): 341-359, Springer, 1997.

[13] A. P. Dempster, N. M. Laird and D. B. Rubin, Maximum likelihood from incomplete data via the EM algorithm. *Journal of the Royal Statistical Society*, Series B, 39(1):1-38, Wiley, 1977.